FEBS Letters

FEBS PRESS science publishing by scientists

REVIEW ARTICLE

From *in vitro* towards *in situ*: structure-based investigation of ABC exporters by electron paramagnetic resonance spectroscopy

Enrica Bordignon[1], Markus A. Seeger[2], Laura Galazzo[1] and Gianmarco Meier[2]

1 Faculty of Chemistry and Biochemistry, Ruhr University Bochum, Bochum, Germany
2 Institute of Medical Microbiology, University of Zurich, Switzerland

Correspondence
E. Bordignon, Faculty of Chemistry and Biochemistry, Ruhr University Bochum, 44801 Bochum, Germany
Tel: +49 (0)234 3226239
E-mail: enrica.bordignon@rub.de
M. A. Seeger, Institute of Medical Microbiology, University of Zurich, Gloriastr 28/30, 8006 Zurich, Switzerland
Tel: +41 (0)44 634 53 96
E-mail: m.seeger@imm.uzh.ch

(Received 19 July 2020, revised 30 October 2020, accepted 15 November 2020, available online 1 December 2020)

doi:10.1002/1873-3468.14004

Edited by: Ute Hellmich

ATP-binding cassette (ABC) exporters have been studied now for more than four decades, and recent structural investigation has produced a large number of protein database entries. Yet, important questions about how ABC exporters function at the molecular level remain debated, such as which are the molecular recognition hotspots and the allosteric couplings dynamically regulating the communication between the catalytic cycle and the export of substrates. This conundrum mainly arises from technical limitations confining all research to *in vitro* analysis of ABC transporters in detergent solutions or embedded in membrane-mimicking environments. Therefore, a largely unanswered question is how ABC exporters operate *in situ*, namely in the native membrane context of a metabolically active cell. This review focuses on novel mechanistic insights into type I ABC exporters gained through a unique combination of structure determination, biochemical characterization, generation of conformation-specific nanobodies/sybodies and double electron–electron resonance.

Keywords: ABC transporters; DEER; detergent; EPR; inside–out vesicles; liposomes; MTSL; nanobody; spin label; sybody

ATP-binding cassette (ABC) exporters fall into two subclasses (type I and type II) and play an important role in the physiology of the human body [1]. According to the Membrane Proteins of Known 3D Structure (mpstruc) database (https://blanco.biomol.uci.edu/mpstruc/), there are currently more than 20 unique type I ABC exporters, the structure of which has been elucidated. For many of the ABC transporters, structures have been determined for closely related homologues (e.g. CFTR [2,3]), multiple conformations (e.g. TM287/288 [4–6], TmrAB [7,8], PglK [9,10], MsbA [11–13] or MRP 1 (ABCC1) [14,15]) or multiple bound substrates and inhibitors (e.g. Atm1 [16] or ABCB1 [17]). Comparatively less is known for type II ABC exporters, which constitute the ABCA and ABCG families of human ABC transporters [18,19], but are also involved in lipid-oligosaccharide export in bacteria [20].

Transported substrates range from xenobiotics (multidrug efflux pumps) over lipids to peptides, while other type I ABC exporters have evolved into ATP-gated chloride channels (CFTR) [21] and regulators of potassium channels (SUR1) [22]. Most recently, two mycobacterial I ABC exporters have been shown to act as importers of siderophores (IrtAB [23]) and vitamin B_{12} (Rv1819c [24]).

Despite the functional diversity, type I ABC exporters, the focus of this review, share the same structural

Abbreviations
ABC exporters, ATP-binding cassette exporters; DEER, double electron–electron resonance; EPR, electron paramagnetic resonance; NBD, nucleotide-binding domain.

fold, suggesting that they also employ a common transport mechanism. Notably, according to the newly proposed nomenclature of ABC transporters, which is based on structural homology of the transmembrane domain, 'type I exporters' have been reclassified as 'type IV' transporters [25]. The transport cycle of the canonical ABC exporters, which actively pump substrates from the cytoplasmic to the extracellular/periplasmic side, entails the following steps: (a) substrate capture typically involving the inward-facing (IF) cavity at the transmembrane domains (TMDs); (b) nucleotide-binding domain (NBD) dimerization completed and sealed by the binding of two ATP molecules and a concomitant reorientation of the substrate-binding cavity; (c) substrate release, involving the opening of the extracellular gate; (d) ATP hydrolysis (generally believed to occur after substrate release, but in principle this may also occur simultaneously or previously to substrate release); and finally v) phosphate release and dissociation of the NBD dimer to reset the transporter back to the IF state (a process intimately coupled to the closure of the extracellular gate; Fig. 1).

Structures are well-characterized fixed points of the transport cycle, but they only describe some of the events that can be stably trapped; other conformations (e.g. during NBD closure or opening) and events (e.g. substrate release or ATP hydrolysis) are intrinsically more dynamic and thus very difficult to characterize at the structural level. Therefore, orthogonal methods are becoming increasingly important to shed light on these important yet largely unexplored steps of the transport cycle.

This review will therefore focus on methodological advances in the field of spectroscopic methods, in particular electron paramagnetic resonance (EPR) spectroscopy. Finally, structural and biochemical elucidation of ABC exporters is almost exclusively performed with purified and often also membrane-reconstituted proteins. However, detergents and membrane mimics cannot fully replicate the native cellular environment. Here, we propagate the use of highly specific affinity reagents (e.g. nanobodies) as tools to study ABC exporters *in situ*.

Electron paramagnetic resonance spectroscopy

Electron paramagnetic resonance is widely applied in the field of ABC transporters as this technique has no limitations in terms of proteins' size or environment. However, it requires the introduction of paramagnetic spin centres in the protein of interest, for example by site-specifically attaching spin labels to cysteines introduced at desired sites, with specificity requiring the replacement of all natural cysteines. The most common spin label is MTSL (1-Oxyl-2,2,5,5-tetramethyl-Δ3-pyrroline-3-methyl) (methanethiosulfonate), a nitroxide label with spin 1/2 [26]. For specific applications, maleimide-functionalized chelated Gd^{3+} spin labels (spin 7/2) [27] were also used in the ABC transporter field, as described in the following. Additionally, it is possible to insert paramagnetic Mn^{2+} ions (spin 5/2) to replace the diamagnetic metal cofactor Mg^{2+}, which coordinates ATP in the NBDs.

The EPR analysis of an ABC transporter can provide three main types of information. First, the rotational dynamics (so-called 'mobility') of the nitroxide-labelled side chains can be monitored at physiological temperature via lineshape analysis [28]. In fact, the features of the continuous-wave EPR spectra encode the ps-ns rotational correlation times of the bound spin-labelled side chains, which can be modified by changes in protein's structure induced for example by binding of nucleotides or substrates. Second, the water or lipid accessibility of the spin-labelled side chains can be measured via relaxation enhancement induced by paramagnetic agents which preferentially partition in specific environments, for example NiEDDA (in water) or molecular oxygen (in lipids) [28–30]. As an example, the site-specific changes in relaxation during the conformational cycle of transporters can be used to follow the opening and closing of water cavities in the TMDs during nucleotide cycle. Water accessibility can also be measured at physiological temperature by overhauser nuclear dynamic polarization [31]. Third and most importantly, distances between two introduced spins can be measured via pulsed dipolar EPR methods. The leading method is double electron–electron resonance (DEER, also called PELDOR) [32]. DEER requires the sample to be frozen and allows detection of mean interspin distances from 1.5 to 6–7 nm in membrane proteins [32,33] (longer distances can be achieved using fully deuterated proteins in fully deuterated media). An advantage of this technique is that distances between the same type of labels (e.g. two nitroxide spins) or between different types of labels (e.g. a Gd^{3+} and a nitroxide label) can be selectively addressed (see, e.g., Ref. [27,34,35]). When spin pairs are introduced in several double cysteine mutants of an ABC transporter, distance constraints can be obtained for different conformational states of the transporter. The distance constraints can be used to validate existing X-ray and cryo-EM structures, to build coarse-grained models of the missing conformations of an ABC transporter via rotamer-based approaches [36] and to unveil

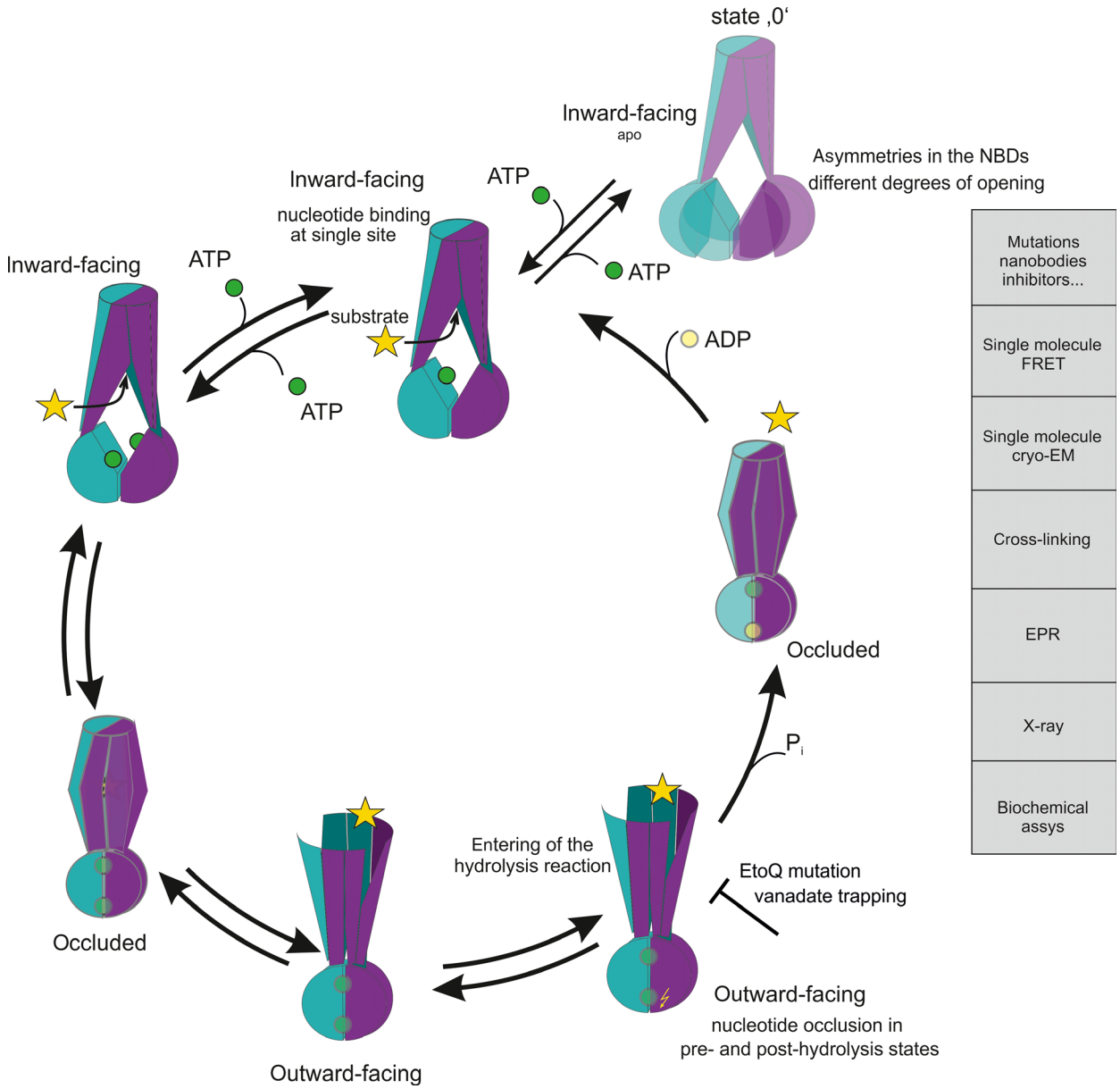

Fig. 1. Transport cycle of type I ABC exporters. Sketch of the conformations characterized *in vitro* by biophysical and biochemical methods. Due to the high ATP concentration in cells, the lifetime of the transporter with empty NBDs (apo-state *in vitro*, state '0') is highly transient, and possibly populated only in homodimeric ABC exporters, when both hydrolysed ATP molecules leave the NBDs. The sketch assumes that one molecule of ATP is hydrolysed per cycle, which had been proposed for both homo- and heterodimeric ABC exporters. In the first part of the cycle (IF-to-OF isomerization), the interconversion between IF/Occ/OF states is reversible. The respective conformational equilibria are transporter-specific. The Occ state with a bound substrate had never been observed in a structure. Once one ATP molecule is committed to hydrolysis at the closed NBDs, the resetting step of the cycle is initiated, which is unidirectional and thus ensures net transport of substrate by preventing substrate re-flux into the cell. Next to ATP hydrolysis, extracellular gate closure plays an important role for NBD opening (Occ state without substrate bound). This representation is valid for most homodimeric, heterodimeric, and single polypeptide transporters (e.g. ABCB1). Substrates and ATP are indicated as stars and green circles, respectively.

conformational equilibria. Notably, after the resolution revolution, single-particle cryo-EM has gained ground in the structural analysis of the energy landscape of ABC exporters (see, e.g., Ref. [8]) and a dedicated review in this issue will deeply address its role in the field.

In the following, EPR-derived insights into structure and dynamics of type I ABC exporters (type IV ABC transporters according to the new nomenclature) are provided.

The ABC exporters' energy landscape

Active substrate transport requires an ABC exporter to alternate between at least two conformations to provide access either towards the inside of the cell to bind substrates (IF) or towards the exterior of the cellular membrane (outward-facing, OF) to expel the substrate once it has translocated through the TMDs (Fig. 1).

Other intermediates have been structurally characterized with different degrees of vicinity between the NBDs and characteristic occluded conformations trapping the substrates before the peristaltic forces in the TMDs expel them. The 'zero' time or initial protein's configuration of such cycle cannot be defined; however, most *in vitro* EPR and other biophysical studies start with the characterization of a resting, apo-state of the transporter in the absence of nucleotides and substrates followed by structural analysis of the changes induced by subsequent addition of nucleotides and substrates or inhibitors (Fig. 1). This resting state may be only very transiently populated in cells, due to the millimolar concentration of cellular ATP [37].

Monitoring the conformational changes that transduce the energy of ATP binding/hydrolysis at the NBDs to the mechanical work of substrate translocation at the TMDs is pivotal to understand the transport mechanism of ABC transporters. EPR is a widely used technique to unveil conformational changes in response to the binding of nucleotides and transport substrates.

The nonhydrolysable ATP analogue AMP-PNP [38] and the slowly hydrolysable ATPγS [39] enable the study of a stable configurational snapshot of the 'ATP'-bound state. AMP-PNP had been successfully used to trap homodimeric ABC exporters such as MsbA in OF conformations with closed NBDs [40,41]. However, in heterodimeric ABC exporters such as TM287/288 [5], TmrAB [42] and BmrCD [38,43], which carry a degenerate and a consensus nucleotide-binding site, or in ABCB1 [44], it was found that the addition of AMP-PNP does not induce the closure of the NBDs, as previously observed also for CFTR [45]. This suggests distinct recognition of this ATP analogue by homodimeric and heterodimeric NBDs.

Next to nucleotide analogues (which are typically added together with magnesium ions), ATP in combination with EDTA had been used to study the effects caused ATP binding, because EDTA chelates all Mg^{2+} ions in the sample and therefore disables ATP hydrolysis [38]. Incubation of the transporter with ATP-Mg finally mimics turnover conditions *in vitro*. Another possibility is to trap the transporter in a high-energy state (HES) or a so-called posthydrolytic intermediate by trapping the ADP–vanadate complex at the NBDs. At present, most biophysical methods, including EPR, made extensive use of nucleotide 'trapping' methods to increase the information content on the different steps in the translocation cycle. The results provide a puzzle of configurations which can then be used to build models of substrate translocation, as sketched in Fig. 1.

Homodimeric exporters

The first EPR-based insights into the conformational transitions of ABC exporters originated from a detailed analysis of a large number of spin-labelled mutants in the homodimeric transporter MsbA by the group of Mchaourab [41]. Being a homodimer, each single cysteine mutant of MsbA produces two spin-labelled side chains symmetric with respect to the symmetry axis of the transporter, which were used to monitor changes in dynamics and water accessibility going from the apo-state to the AMP-PNP and ATP–vanadate states. The transition from an IF to an OF state could be directly inferred from the EPR analysis at physiological temperature in proteoliposomes. The effects induced by AMP-PNP were found to be accentuated by trapping of the posthydrolytic transition state with vanadate. The authors stated that 'ligand-free MsbA samples conformations that depart from the crystal structures' [41], but at that time, only the erroneous (and later retracted) apo-state structure of MsbA was available [46]. Hence, the site-specific information obtained by EPR was in fact accurately representing the correct conformation of apo-MsbA. Side-chain dynamics and interspin distances also proved that the addition of LPS to MsbA induced pronounced structural rearrangements possibly reflecting a solvent-like effect in the apo-state [47] and that mutations in the catalytic glutamate (E506Q) or in the H-motif (H537A) decrease the NBD separation even in the absence of nucleotides [48].

The OF structure of MsbA found by EPR to be populated by both addition of AMP-PNP-Mg and vanadate trapping in detergent-solubilized and lipid-reconstituted MsbA illuminated a two-state alternate-access mechanism for substrate translocation (Fig. 2A). Notably, the consistent EPR distance constraints measured in the OF state of MsbA in different

laboratories [40,49] are in perfect agreement with the first OF crystal structure of a bacterial ABC transporter (Sav1866) published by Dawson and Locher in 2006 [50] and the subsequent OF structure of MsbA [11]. The known OF structures of the homodimeric transporters are structurally symmetric. However, biochemical evidence suggests that in the homodimeric transporter BmrA, only one ATP molecule per homodimer is trapped by vanadate or by the EtoQ mutation, indicating that, despite the symmetric nature of the NBDs, asymmetries are generated during the hydrolysis cycle [51]. This was also shown for MsbA with the help of DARP in binders [40].

Interestingly, the EPR data in detergent and liposomes [40,49] fully support the controversially discussed apo-crystal structure of MsbA featuring a widely opened IF conformation [11]. Interestingly, a more recent single-particle cryo-EM structure of MsbA obtained in nanodiscs suggests that the apo-state adopts an IF conformation with the NBDs in closer distance [11], in line with single-molecule FRET data detected in nanodiscs [52]. In contrast, DEER analysis of MsbA reconstituted in another type of nanodiscs confirmed the large separation of the NBDs seen in liposomes [53]. The dynamic nature of the apo-state of another detergent-solubilized homodimeric transporter, namely LmrA, was confirmed by DEER. In analogy to MsbA, a stable OF conformation of LmrA was induced by ATP binding [54].

In conclusion, DEER data pertaining to the OF state of homodimeric exporters are in agreement with the available structures of Sav1866 and MsbA. However, the degree of NBD separation in the absence of ATP in the context of the lipid bilayer remains a matter of debate.

Heterodimeric exporters and ABCB1

In the following chapter, we compare the structural findings obtained by EPR on the energy landscape of three heterodimeric bacterial transporters (BmrCD, TmrAB and TM287/288) and on ABCB1 (or Pgp).

The main characteristic of the heterodimeric transporters is the existence of a canonical ATP-binding site, which is capable of ATP hydrolysis, and of a degenerate binding site, in which ATP hydrolysis is strongly impaired or does not even occur [4,55]. Using EPR, asymmetric ATP hydrolysis by the two nucleotide-binding sites of the heterodimeric transporter BmrCD was in fact directly detected by analysing the coordination sphere of the Mn^{2+} cofactor in the nucleotide-binding sites, which replaces the Mg^{2+} [56]. ABCB1, despite having two nucleotide-binding sites competent for ATP hydrolysis, was early recognized to hydrolyse only one ATP per catalytic cycle, highlighting asymmetries in the conformational transitions [57], which could share some structural analogies with the heterodimeric transporters.

In 2012, the crystal structure of the heterodimeric ABC transporter TM287/288 from the hyperthermophilic bacterium *Thermotoga maritima* was solved in its IF state, with the NBDs only partially separated, remaining in contact through an interface involving conserved motifs that connect the two ATP hydrolysis sites [4]. Intriguingly, AMP-PNP was bound to the degenerate catalytic site, which deviates in TM287/288 from the consensus sequence in the same positions as the eukaryotic homologs CFTR and TAP1/2. The fact that TM287/288 assumed its IF state despite the addition of AMP-PNP for crystallization raised the question whether heterodimeric transporters may have different nucleotide requirements to stabilize the OF state than homodimeric ABC exporters such as MsbA. DEER analysis of several spin-labelled pairs introduced in TM287/288 either solubilized in detergent or reconstituted in liposomes confirmed that the apo-state adopts an IF state with NBDs in closer contact than the homodimeric MsbA, and that addition of AMP-PNP-Mg does not induce closure of the NBDs, in stark contrast with MsbA [58].

Concomitant with these findings, an EPR study on heterodimeric BmrCD (from the mesophilic bacterium *Bacillus subtilis*) either solubilized in detergent or reconstituted into nanodiscs revealed an asymmetry in the apo-state of the transporter in the two ATP-binding sites nucleotide-binding sites 1 and 2 (NBS1 and NBS2) as mapped by two pairs of spin labels. The consensus site was more flexible than the degenerate site, and addition of AMP-PNP-Mg stabilized an IF conformation with NBDs in close contact, reminiscent of the TM287/288 IF state [43]. We showed that ATP-γ-S-Mg has the same effect as AMP-PNP-Mg and ADP-Mg in BmrCD, whereas ATP-EDTA did not induce the IF conformation with the NBDs in contact, nor the OF conformation (Fig. 2B) [38]. The OF state of BmrCD could only be stabilized in the presence of ATP–vanadate (Fig. 2B). Based on these findings, it was suggested that ATP hydrolysis represents the essential power stroke for the IF-OF isomerization of heterodimeric type I ABC exporters [43]. Interestingly, TM287/288 had very similar features as BmrCD when incubated at high temperatures (80 °C) before being shock-frozen for DEER analysis [38]. In fact, in the absence of nucleotides the consensus site (but not the degenerate site) was found to be dynamically uncoupled from the TMDs. The addition of AMP-PNP at

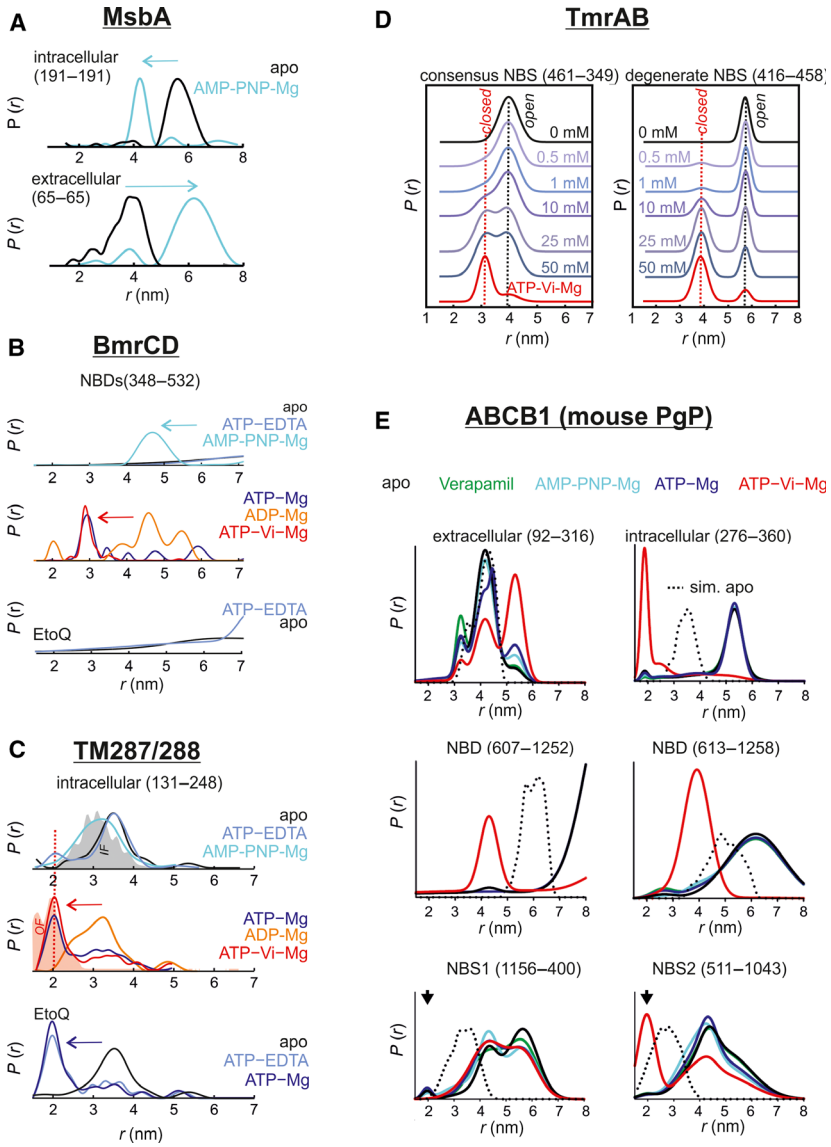

Fig. 2. Interspin distances obtained by DEER unveil the conformational transition of ABC exporters. (A) Interspin distances between pairs of MTSL spin labels introduced in the intracellular and extracellular region of MsbA in the apo- and AMP-PNP-Mg-bound state (adapted from Ref. [40]).Data are consistent with [49]. (B) BmrCD shows large separation between the NBD pair of MTSL spin labels in the apo-state. ATP-EDTA does not induce the formation of closed NBDs. AMP-PNP-Mg brings the NBDs in contact, with the structure resembling the IF state of TM287/288 in the AMP-PNP-bound state. Under turnover conditions, there is a fraction of OF state present, with NBDs tightly closed, together with conformations with NBDs largely dissociated. ADP-Mg induces an IF conformation with NBDs in contact. The E592Q mutation in BmrD shifts the population to the OF state in the presence of ATP-Mg (adapted from Ref. [38]). Ddata are consistent with Ref. [43]. (C) The DEER analysis of TM287/288 identifies an apo-state with NBDs in contact, in line with the crystal structure (shaded areas represent the interspin distances simulated with the rotamer library available in the software MMM [36]). The addition of AMP-PNP-Mg has no structural effects. The addition of ATP-EDTA is sufficient to create an IF/OF equilibrium, in contrast to BmrCD. Under turnover conditions, both IF and OF states are present. Vanadate trapping shifts the population to the OF state, as in BmrCD. The EtoQ mutation at the consensus site shifts the population to the OF state in the presence of both ATP-EDTA and ATP-Mg (adapted from Ref. [38]). (D) The DEER analysis performed on TmrAB highlights the analogies with TM287/288. The IF/OF equilibrium induced by ATP-EDTA is shown here to be dependent on the ATP concentration (adapted from Ref. [42], data kindly provided by B. Joseph). (E) DEER analysis on mouse Pgp (reproduced with permission from Ref. [44]). The apo-configuration shows asymmetries in the NBDs, as in BmrCD and TM287/288 (at high T), and the distances often have average distances larger than those simulated on the mouse Pgp crystal (4M1M, dotted lines). The addition of AMP-PNP does not induce the OF conformation. Under turnover condition (ATP-Mg in the presence of verapamil), the transporter adopts predominantly the IF conformation, different from BmrCD, TmrAB and TM287/288. The HES, also called posthydrolytic intermediate trapped with vanadate, switches the conformation to the OF state. The extracellular region is disordered, as in TM287/288. Asymmetries are found in the A-loop of the NBSs 1 and 2.

high temperature stabilized the IF conformation with contacting NBDs, as in BmrCD [38]. Therefore, at their physiological temperatures, both heterodimeric transporters had similar properties and in both cases AMP-PNP did not induce the IF-to-OF switch, but only stabilized an IF conformation with NBDs in contact. Under turnover conditions, both BmrCD and TM287/288 showed similar fractions of OF and IF conformations, indicating that the energy profile of both transporters is similar.

In TM287/288 and TmrAB, the addition of ATP-EDTA induced an equilibrium between IF and OF states of the transporter, while trapping of the posthydrolytic transition state intermediate with vanadate was needed to fully enrich the population of the OF conformation in the ensemble (Fig. 2C,D). These findings unveiled that ATP binding is sufficient to trigger the formation of the OF state in these heterodimeric transporters [38,42]. The existence of such IF/OF equilibrium possibly enabled monitoring the IF-Occ-OF conformational transition of TM287/288 *in silico* via molecular dynamic simulations [59]. In a recent study, thermodynamic parameters of the ATP-driven IF-OF transition of TmrAB were studied by DEER, revealing a high-energy barrier separating the two states resulting in slow kinetic interconversion between them [60]. TmrAB has been shown to be a human antigen transporter ortholog [7] capable of exporting peptides. Interestingly, the addition of high peptide concentrations to TmrAB inhibits its ATPase activity by inducing an occluded (Occ) conformation, as shown by DEER [42]. In the presence of ADP-Mg, the three heterodimeric transporters showed an IF conformation similar to the AMP-PNP state [38,42,43]. In conclusion, all heterodimeric ABC transporters investigated up to now do not respond to AMP-PNP by switching to the OF state; rather, this nucleotide analogue stabilizes an IF conformation with NBDs in partial contact. The addition of ATP is required to populate the OF state in two investigated transporters (TM287/288 and TmrAB), yet one transporter (BmrCD) did not respond to ATP-EDTA. However, under turnover conditions (ATP-Mg), a large fraction of OF conformations was present in both TM287/288, and BmrCD and TmrAB [38,42,43].

Analogously to the effects induced by vanadate trapping, the introduction of the EtoQ mutation in the consensus site of TM287/288 and TmrAB, which traps the ATP in a prehydrolytic configuration, moved the equilibrium towards the OF state [38,60] (Fig. 2C). The extracellular gate was found to be disordered in TM287/288 and BmrCD (with distances characteristic of both the closed conformation and open conformation in equilibrium in the vanadate-trapped state) [38,43] and more open in the case of TmrAB under the same experimental conditions [42], highlighting at diversities in terms of gate dynamics through which the substrates are expelled. The existence of an IF/OF equilibrium in some heterodimeric transporters poses the question whether it is possible to run the machinery back and forth, with a bidirectional substrate transport. However, the unidirectionality of transport is ensured by the fact that once primed for ATP hydrolysis, the transporter irreversibly proceeds with hydrolysis, and the IF state is restored (Fig. 1). In support of this notion, the lifetime of the ATP-trapped OF state of TM287/288 carrying the EtoQ mutation is highly similar to the low residual ATPase activity of this mutant. This means that once ATP is trapped tightly at the NBDs, ATP hydrolysis needs to occur first before the cycle continues [6]. It was further shown that extracellular gate closure is important for active transport by the TM287/288 homologue EfrEF and that a tightly sealed extracellular gate is pivotal for NBD opening during the resetting step [6]. Hence, the intricate coupling between ATP hydrolysis, extracellular gate closure and NBD opening prevents back flux of the substrates and ensures unidirectional uphill transport.

The properties unveiled for the heterodimeric ABC exporters have striking similarities and some differences with respect to ABCB1 (or PgP; Fig. 2E), which plays a central role in the clearance of xenobiotics and in cancer resistance to chemotherapy. Mouse ABCB1 was extensively characterized by DEER [44,61]. In the apo-state, the intracellular region of ABCB1 shows mean distances larger than those expected by modelling the spin labels on the mouse Pgp crystal structure [62], suggesting a more open IF conformation similar to that observed in the *Caenorhabditis elegans* Pgp structure [63]. A striking analogy with the heterodimeric transporters is that AMP-PNP cannot induce the OF state in ABCB1 and that vanadate trapping is the most efficient way to populate effectively the OF state [44]. A distinct feature of ABCB1 is that, under ATP turnover conditions, the population of the OF state is close to the DEER detection limit, indicating that the IF state for ABCB1 is energetically favoured, and the OF state is only transiently populated. This effect could be in principle induced by the freezing of the samples; however, in all other exporters frozen under the same conditions the OF state could always be trapped. Another reason for the destabilization of the OF state could be the environment (lipids, detergent–lipid mixtures or nanodiscs), and this should be further investigated. The extracellular region of

ABCB1 samples both closed and open conformations in the vanadate-trapped state, akin to TM287/288 and BmrCD. Intriguingly, the A-loops were found to be highly asymmetric in ABCB1 in the vanadate-trapped state and the intrinsic local asymmetry at the NBSs is suggested to reflect catalytic asymmetry. The A-loop asymmetries were found to be modulated by substrates and inhibitors, suggesting that substrate-induced acceleration of ATP hydrolysis correlates with stabilization of structurally asymmetric nucleotide-binding sites [61]. Analogously to what found for TM287/288, when both EtoQ mutations are present in ABCB1 (prehydrolysis conditions), there is a shift towards the OF state in the presence of ATP-Mg.

DEER studies of type I ABC exporters support the notion that ABC transporters are molecular machines whose energy landscape is shaped by ATP, substrates and possibly lipids in a plastic manner to ultimately couple unidirectional transport to the hydrolysis of ATP.

Sybodies and nanobodies as affinity reagents for structural investigation of ABC exporters

ABC exporters have been the target for antibodies and antibody fragments for many decades. Motivated by the prospect of inhibiting ABCB1 and thereby overcoming cancer-related multidrug resistance, the mouse antibodies UIC2 and MRK16 were generated [64,65]. Recent cryo-EM studies showed that UIC2 binds to an extracellular epitope of ABCB1 and its binding results in a loss of ABCB1-mediated drug resistance in cancer cells by preventing the opening of ABCB1's extracellular gate [66]. This finding is in line with surface plasmon resonance measurements showing that the affinity of both UIC2 and MRK16 is decreased when ABCB1 is trapped in its posthydrolysis state using ATP–vanadate, which results in extracellular gate opening [67]. The homodimeric ABCB1 homologue CmABCB1 was targeted by an *in vitro* selected macrocyclic peptide called aCAP [68]. A 2.4 Å crystal structure revealed that akin to the human ABCB1 antibody UIC2, aCAP prevents the opening of the extracellular gate, but in contrast to UIC2, ATPase activity was found to be strongly reduced [69]. ABCB1 was also the target of single-domain antibodies generally known as nanobodies; a nanobody binding to the NBD1 prevents NBD closure and thereby inhibits ATPase activity [70]. Designed ankyrin repeat proteins (DARPins) raised against the heterodimeric bacterial multidrug efflux pump LmrCD were found to increase resistance towards daunorubicin by threefold; hence, some binding proteins have the capacity to stimulate the pumping activity of ABC exporters [71]. A DARPin raised against homodimeric MsbA was found to bind in a ratio of one DARPin per homodimer, thus stabilizing an asymmetric conformation of this transporter. Interestingly, asymmetric trapping of MsbA resulted in a twofold increased ATPase activity [40]. Asymmetric binding was also observed for a nanobody recognizing homodimeric PglK; due to subtle asymmetries that did not become obvious in a 3.9 Å crystal structure, only one nanobody binds to the NBDs of PglK and thereby inhibits ATPase activity by acting as a sticky doorstop [72]. While inhibitory binders explained above all prevent the isomerization from the IF to the OF state, we recently generated synthetic nanobodies known as sybodies against the heterodimeric ABC exporter TM287/288 with the aim to stabilize the OF conformation [6,73,74]. We took advantage of the fact that sybodies are selected entirely *in vitro* and performed the selections in the presence of saturating ATP concentrations and TM287/288 carrying the Walker B EtoQ mutation [38]. Using surface plasmon resonance (SPR) as read-out, we identified more than 10 sybodies exhibiting various degrees of conformational preference for the OF state. A crystal structure of a highly OF state selective sybody (Sb_TM#35) showed that it binds to one of the extracellular wings and acts as a clamp (Fig. 3). In the same study, two alpaca nanobodies binding to the NBDs of TM287/288 were also described. These nanobodies were generated by immunizing an alpaca with TM287/288 cross-linked in an OF conformation. One of the nanobodies (Nb_TM#1) recognized an epitope that only forms when the NBDs are fully closed and was like the sybody specific for the OF conformation. In contrast, the second nanobody (Nb_TM#2) bound sideways to the NBD288 (Fig. 3) and did not have any preference for the IF or OF state as judged from SPR [6]. Sybody- and nanobody-induced effects on the conformational equilibria were studied by DEER, using spin-labelled variants of the transporter [6,75]. Figure 3 shows that in the presence of ATP-EDTA, the equilibrium between the IF and OF state is manifested by the appearance of two peaks in the distance distribution, corresponding to the interspin distances predicted by rotamer analysis using the respective crystal structures (shaded areas in Fig. 3). When the state-specific sybody Sb_TM#35 is bound to the extracellular region of TM287/288, the equilibrium is shifted almost completely to the OF state, clearly seen by the change in the ratio between the intensity of the two distance peaks. In contrast, the non-state-specific nanobody Nb_TM#2 did not modify the equilibrium.

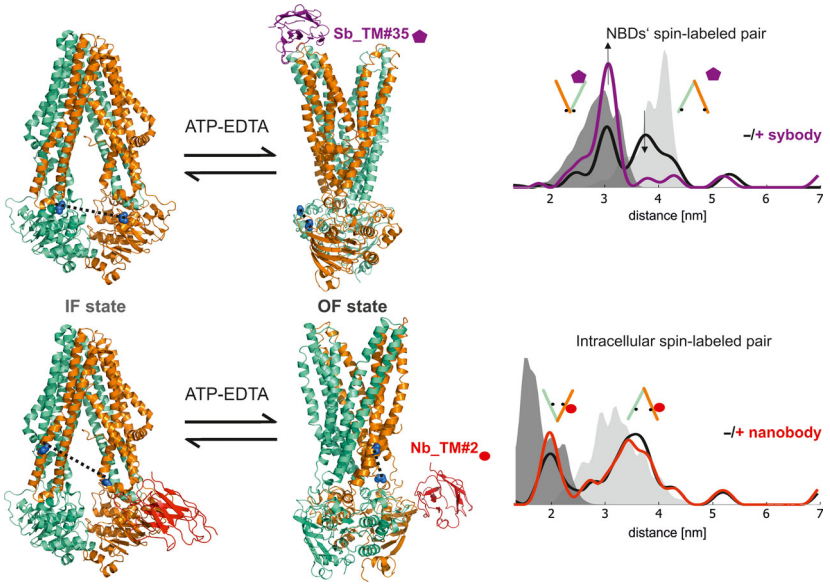

Fig. 3. Sybodies and nanobodies targeting ABC exporters. Left panel: Crystal structures of the detergent-purified TM287/288 in the IF state (PDB file: 4Q4H, with docked Nb_TM#2 in the lower panel) and OF state (PDB files: 6QV0 and 6QV2 for bound Sb_TM#35 and Nb_TM#2, respectively). Spin-labelled positions at the NBDs or in the intracellular region highlighted as blue spheres. In the presence of the nucleotide ATP-EDTA, there is an equilibrium between the two conformations. Sb_TM#35 (in purple) binds to the extracellular region of the transporter only in the OF state, while Nb_TM#2 (in red) binds to NBD288 regardless the presence or absence of ATP. Right panel: Experimental distance distributions for the two pairs shown on the left panel in the absence (–) or in the presence (+) of the sybody/nanobody and corresponding distance predictions based on a rotamer library for IF (light grey) and OF (dark grey) as shaded areas. The data show a complete shift in the IF/OF equilibrium subsequent to the binding of Sb_TM#35.

While most studies have focused on conformation-specific binders with the aim to trap and thereby inhibit ABC exporters, the generation of binders that do not influence the transport cycle and thus can serve as spin-labelled reporter molecules are equally important. Next to the state-unspecific TM287/288 nanobody Nb_TM#2, some of the LmrCD-specific DARPins [71] and the TmrAB-specific nanobody [8] did not influence ATPase activity of the ABC exporters. Hence, it seems possible to routinely isolate binders that are 'inert' in the sense that they bind without modulating the energy landscape of the transporter.

Studying the transporter in different environments: challenges and opportunities

Purification and characterization of ABC transporters with mild detergents were used to be the gold standard to study these proteins *in vitro* at the biochemical and structural levels. While detergents usually are applied as necessary first step for membrane protein extraction from biological membranes, they potentially destabilize and thereby may impair the function of the investigated protein (Fig. 4). Membrane mimetics such as nanodiscs or proteoliposomes rely on detergent purification of transporters prior to reconstitution [76,77] (Fig. 4). ABC transporters such as MsbA often show a higher ATPase activity and increased stability when reconstituted in nanodiscs or proteoliposomes as compared to detergent solution [78]. The lipid composition of nanodiscs and proteoliposomes can be tightly controlled to match the native membrane by using lipid mixtures extracted from native source organisms. Nanodiscs have recently been extensively used for structure determination by cryo-EM, producing sample specimens that reflect the native lipid context of membrane proteins [12,17]. The size of nanodiscs is mainly determined by the length of the membrane scaffolding protein (MSP) for which several variants are available, yielding nanodiscs of varying diameters [79]. Reconstitution into proteoliposomes is another well-established technique, which is mostly used for the detailed investigation of transport processes across the lipid bilayer [76]. Proteoliposome diameters are made uniform after transporter reconstitution by extruding the specimen through polycarbonate filters with a defined pore size. In contrast to nanodiscs, proteoliposomes exhibit a membrane curvature similar to that in intact cells. While proteoliposomes, nanodiscs and other

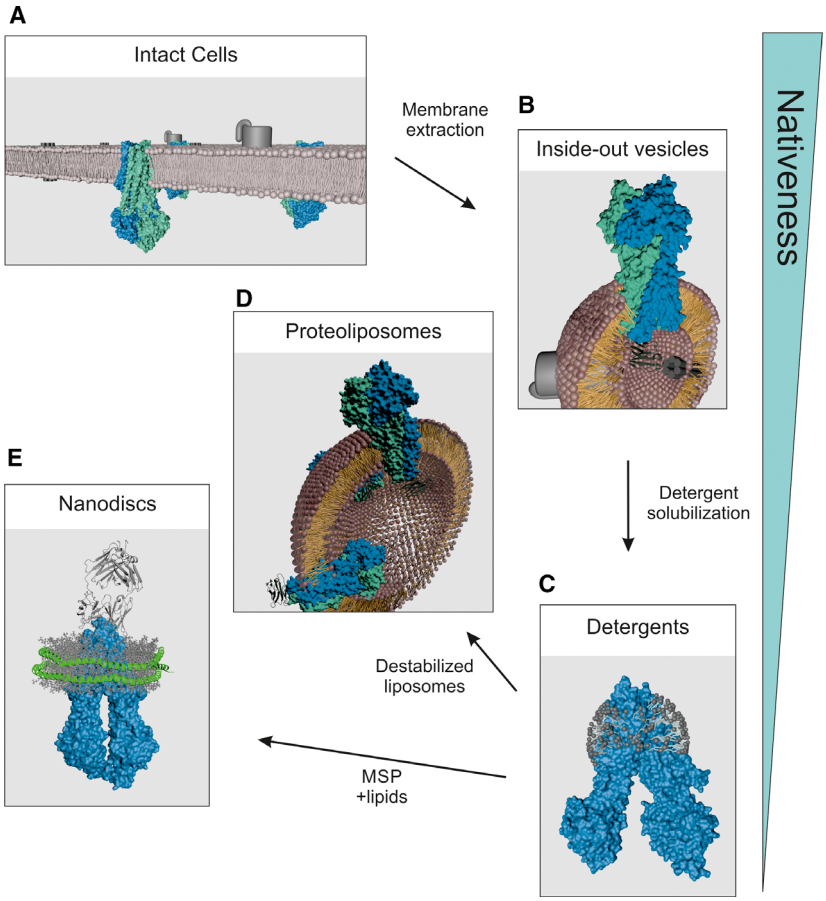

Fig. 4. Experimental investigation of ABC transporters *in situ* and *in vitro*. (A) MsbA (PDB 5TTP) embedded in the lipid bilayer of an intact cell. Note that the membrane is densely populated by other membrane proteins (grey shapes). (B) TM287/288 (PDB 6QV0) shown in the context of a cell-derived ISOV containing other membrane proteins as well. (C) Purified MRP1 (PDB 5UJ9) after detergent solubilization. The detergent forms a belt that shields the transmembrane helices. (D) TM287/288 (PDB 6QV0) reconstituted into proteoliposomes. In this case, the target protein is the only protein in the membrane, and typically, membrane protein density is much lower than in ISOVs. Of note, the reconstituted membrane protein is inserted in both orientations. (E) Structure of ABCB1 (PDB 6QEX) in complex with a Fab fragment after reconstitution into nanodiscs.

membrane mimetics not mentioned here offer the advantage to study a single, purified membrane transporter in the context of a lipid bilayer, they lack the crowded membrane protein environment. In inside–out vesicles (ISOVs) directly extracted from intact cells, this crowding effect is maintained, but ISOVs still lack the (crowded) cytosolic environment and the electrochemical potential found in cells (Fig. 4). Furthermore, membrane curvature is inversed in ISOVs with respect to the intact cell. Therefore, to truly understand the function of an ABC transporter in its native context, there is no perfect experimental substitute other than conducting functional, biochemical and structural studies in metabolically active cells.

Several biophysical techniques are available, which can probe ABC transporters in detergent solution, membrane-mimicking environments, near-native membranes (ISOVs) and intact cells. However, the more native the system becomes (Fig. 4), the less options it offers for biochemical and structural investigations, as outlined in the following and summarized in Table 1.

X-ray crystallography can yield high-resolution structures of membrane proteins in detergents, aiding the characterization of the biophysical foundations of nucleotides' and substrates' recognition. The main bottleneck of X-ray crystallography is the difficulty in generating well-diffracting crystals. To facilitate the crystallization process, state-specific binding proteins such as nanobodies, sybodies or fragment antigen-binding (Fab) antibodies are often used [6,72].

The main advantage of cryo-EM over X-ray crystallography is that by fast freezing of the sample, multiple coexisting conformations can be observed with only comparatively small amounts of starting material. In the recent years, cryo-EM studies of ABC transporters reconstituted in nanodiscs have been reported [8,17], extending the range of environments that can be investigated with this technique.

In the ABC transporters field, solid-state NMR is less used, due to the high molecular weight of these proteins that makes spectra assignment very challenging [80,81]. However, NMR has been used to follow in real time the hydrolysis of ATP [82], and it enabled the discovery that MsbA, LmrA and TmrAB can couple ATP hydrolysis to an adenylate kinase activity, where ADP is converted into AMP and ATP [83].

Table 1. Different environments offer complementary opportunities to study ABC transporters.

Environment	Biochemical assays	Detergent purification	Lipid environment	Size control	Membrane Curvature	Electrochemical gradient	Suitable for X-ray	Suitable for cryo-EM[a]	Suitable for FRET	Suitable for EPR
Detergent	Yes	Yes	No	Limited	No	No	Yes	Yes	Yes	Yes
Nanodiscs	Yes	Yes	Yes	By MSP	No	No	No	Yes	Yes	Yes
Proteoliposomes	Yes	Yes	Yes	By extrusion	Yes	Yes[b]	No	No	Yes	Yes
ISOVs	No	No	Yes	Limited	Yes	Yes[c]	No	No	Potentially[d]	Yes[d]
Cells	No	No	Yes	Fixed size	Yes	Yes	No	No	Potentially[e]	Potentially[e]

[a]Single particle; [b]Electrochemical gradient of proteoliposomes can be established by pH shift of external buffer and the use of the K^+-pore valinomycin; [c]Electrochemical gradient of the lipid bilayer of ISOVs can be generated by the addition of ATP from the outside (proton-pumping by F_1F_0-ATPase); [d]Requires spin- or FRET-labelled affinity reagents or incorporation of unnatural amino acids in the transporter; [e]Has not been shown yet but is in principle possible. Would require spin- or FRET-labelled affinity reagents.

Fluorescence techniques, especially single-molecule FRET, are also employed in the study of ABC transporters [84,85] and they can be carried out at room temperature, removing possible alterations in the protein conformation due to the freezing of the sample. FRET can provide information on the conformations populated in an ensemble in different environments, and by using single-molecule techniques (sm-FRET), it is in principle possible (but highly challenging), to achieve a temporal resolution in the conformational cycle of ABC exporters induced by nucleotides and substrates. Similarly to FRET, it is possible to measure distances between spin labels attached to membrane proteins inserted in different environments using pulsed EPR dipolar techniques. Spin labels are in general smaller than fluorophores used for FRET and therefore less perturbing. To measure interspin distances, the sample needs to be frozen to avoid averaging of the dipolar interactions by molecular tumbling. The lipidic environment is easily accessible to DEER, although the signal-to-noise ratio is in general worse than in detergent due to lower achievable concentration and faster spin relaxation.

Nanodiscs have raised particular interest in the recent years as membrane-mimicking environments for the study of transporters in the presence of nucleotides and substrates or inhibitors by DEER [61], and they offer the perfect environment also for single-molecule cryo-EM, which allows fast screening of different conformations of a transporter and of structural effects induced by substrates and inhibitors (see, e.g., Ref. [17,66]). Intriguingly, in the case of the homodimeric exporter MsbA, cryo-EM [12] and single-molecule FRET [52] studies in nanodiscs recently showed a close distance between the NBDs in the absence of nucleotides. This information is not corroborated by DEER data showing an apo-conformation almost indistinguishable from that in proteoliposomes or detergent micelles [53]. It is worth mentioning that the nanodisc composition in the DEER study was quite different from that used in cryo-EM; however, the existing discrepancies open the hypothesis of a conformational dependency on the nanodisc preparation and composition.

Ideally, an ABC transporter should be investigated in the native cellular membrane. Biochemical assays can be performed in near-native environments such as ISOVs (e.g. cross-linking, ATPase activity [86]), but they cannot provide structural information at a molecular level.

In the recent years, the introduction of biocompatible spin labels based on gadolinium ions (Gd^{3+}) [27,87–93] has led to major progress in the field of in-cell EPR. Spin-labelled recombinantly produced soluble proteins have been already introduced into cells at micromolar concentrations using electroporation methods and interspin distances could be successfully detected (see, e.g., Ref. [94–96]). Sterically shielded nitroxide labels were also developed that have an increased lifetime in the reducing cellular environment [97–105].

An additional route which is under investigation in the field is the use of genetically encoded unnatural amino acids carrying a functional group for *in situ* labelling or directly a spin-labelled probe [106–111].

However, up to now, spin labelling techniques targeting membrane proteins in cellular environments were successfully applied only to outer membrane proteins of *Escherichia coli* [112–115], but methods to label a membrane protein in the inner membrane of *E. coli* or in the cellular membranes of mammalian cells have not yet been established.

Nanobody-assisted *in situ* EPR

Our groups have recently developed a nanobody-based approach, which offers an elegant alternative for *in situ* studies of membrane proteins.

The conceptual idea behind this approach is to use spin-labelled nanobodies as probes, which then enable the characterization of the conformational landscape of wild-type ABC transporters or biomedically interesting mutants directly in their native environment.

The nanobody selection is a crucial step in this method, and to optimize the choice of the nanobody for the intended study, it is desirable to know its relative position with respect to the transporter. Single-particle cryo-EM can provide relatively quickly the architecture of the complex at a sufficiently high resolution. Once the nanobody binding site is known, the nanobody can be docked to other structural models of the transporter and then simulate the fingerprint inter-nanobody distance for each existing conformation of the transporter. Ideally, the spin-labelled nanobody reporter should be inert with respect to the ATPase activity and substrate transport of the targeted ABC transporter and should not perturb conformational equilibria, in order to read out the native conformational landscape of the target protein.

A prerequisite for nanobody-assisted in-cell EPR is the intracellular delivery of a sufficiently high amount of nanobodies. This can be achieved by electroporation with high-voltage electrical pulses that generate transient pores through which the nanobodies are taken up. For mammalian cells and for Gram-negative bacteria, electroporation proved to be very efficient for small proteins below 30 kDa (nanobodies have a molecular weight of around 15 kDa) [94]. Electroporation has also been applied to Gram-positive bacteria, but the thick peptidoglycan layer limits efficient protein delivery.

In our recently published nanobody-assisted EPR study [75], we used a 'cocktail' of a state- and a non-state-specific nanobody to probe the conformation of the heterodimeric exporter TM287/288 in the membrane environment of ISOVs using DEER spectroscopy. Due to the specificity of the nanobodies, only TM287/288 was targeted in the crowded membrane environment of the ISOVs. As proven by *in vitro* control experiments, using one nanobody which binds with high affinity to the transporter only in the OF state (orange nanobody in the artistic view in Fig. 5) and one which binds to both IF and OF states (yellow nanobody), we created an experimental system in which inter-nanobody distances arise only from the fraction of transporters that shows closed NBDs. This method allowed monitoring the closure of the NBDs of wild-type TM287/288 in ISOVs (Fig. 5).

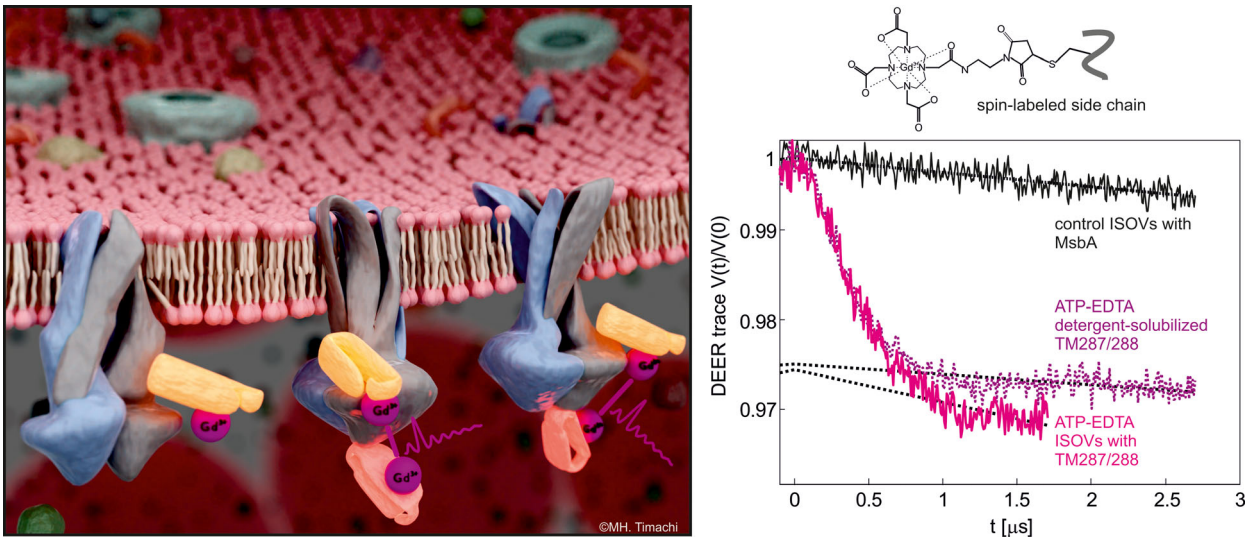

Fig. 5. Nanobody-assisted *in situ* EPR. Left panel: artistic representation of the *Escherichia coli* inner membrane, with the transporter TM287/288 in the IF and OF states. The nanobodies Nb_TM#1 and Nb_TM#2 are shown in neon colours and the Gd-maleimide-DOTA label as purple spheres. As only Nb_TM#2 is bound in the IF state, a dipolar coupling between the two nanobodies is present only when the NBDs are closed, allowing the detection of a DEER trace (purple). Right panel: on the top, chemical structure of the Gd-maleimide-DOTA label bound to a cysteine. At the bottom, primary DEER traces in the presence of ATP-EDTA in detergent (light purple, dashed) and in ISOVs (purple, solid line). The high similarity between the two DEER traces indicates comparable inter-nanobody distances between Nb_TM#1 and Nb_TM#2 in the two environments. However, the shorter DEER trace in ISOVs with respect to detergent does not allow the same accuracy in the distance distribution, which should be optimized in future studies. As a control (grey), ISOVs containing the homodimeric exporter MsbA were also incubated with the two nanobodies. The absence of a dipolar modulation proves the specificity of the binding of the two nanobodies to TM287/288.

However, we realized that the chosen pair of nanobodies used in our pioneering study had two major shortcomings, which should be avoided in the future. First, the pair of nanobodies gave rise to a DEER signal only for the conformations with closed NBDs (i.e. OF and Occ) but was unable to probe the IF state. For future studies, we therefore will focus on nanobodies which are not conformation-specific. Second, our TM287/288 shifts the conformational equilibriums towards the OF state and thus do not act as true reporters as they perturb the measurement. Therefore, it is important to identify 'inert' nanobodies, which do not influence the energy landscape of the targeted ABC transporter and provide useful inter-nanobody distance information to reliably monitor conformational changes.

Conclusions and perspectives

Nanobody-assisted EPR is not free of disadvantages, but it nevertheless opens exciting possibilities for the study of ABC transporters and other molecular machines in their native environment. Furthermore, it provides a powerful tool to compare the conformational transitions in an ensemble of wild-type transporters in different environments from *in vitro* to *in situ*, and possibly also in the cell. Towards this goal, our proof-of-principle made use of a biocompatible Gd-based spin label, as the presence of reducing agents in a cellular milieu will prevent the use of the more commonly employed nitroxides. Notably, ISOVs can also show a residual presence of reducing agents, justifying the choice of a bioresistant spin label for this type of environment as well.

The high specificity of the nanobody is the key element paving the way for in-cell applications. Additionally, the same nanobody used for EPR can also be labelled with fluorophores to monitor via super-resolution microscopy the correct localization of the reporters within a cell.

To be successful in cells, nanobody-assisted DEER requires an optimal control of the transporters' expression levels in a cell and of the amount of inserted nanobodies via electroporation methods. Despite the unavoidable heterogeneities in both protein expression and cellular nanobody uptake, one needs to achieve an average stoichiometric ratio close to two nanobodies per transporter for optimal signal-to-noise ratio in a DEER experiment. In-cell nanobody-assisted EPR will be the next milestone to achieve a deeper understanding of the transporter's conformational landscape in native environments.

Acknowledgements

Open access funding enabled and organized by Projekt DEAL.

References

1 Srikant S and Gaudet R (2019) Mechanics and pharmacology of substrate selection and transport by eukaryotic ABC exporters. *Nat Struct Mol Biol* **26**, 792–801.
2 Zhang Z and Chen J (2016) Atomic structure of the cystic fibrosis transmembrane conductance regulator. *Cell* **167**, 1586–1597.e9.
3 Zhang Z, Liu F and Chen J (2017) Conformational changes of CFTR upon phosphorylation and ATP binding. *Cell* **170**, 483–491.e8.
4 Hohl M, Briand C, Grütter MG and Seeger MA (2012) Crystal structure of a heterodimeric ABC transporter in its inward-facing conformation. *Nat Struct Mol Biol* **19**, 395–402.
5 Hohl M, Hürlimann LM, Böhm S, Schöppe J, Grütter MG, Bordignon E and Seeger MA (2014) Structural basis for allosteric cross-talk between the asymmetric nucleotide binding sites of a heterodimeric ABC exporter. *Proc Natl Acad Sci USA* **111**, 11025–11030.
6 Hutter CAJ, Timachi MH, Hurlimann LM, Zimmermann I, Egloff P, Goddeke H, Kucher S, Stefanic S, Karttunen M, Schafer LV *et al.* (2019) The extracellular gate shapes the energy profile of an ABC exporter. *Nat Commun* **10**, 2260.
7 Noll A, Thomas C, Herbring V, Zollmann T, Barth K, Mehdipour AR, Tomasiak TM, Bruchert S, Joseph B, Abele R *et al.* (2017) Crystal structure and mechanistic basis of a functional homolog of the antigen transporter TAP. *Proc Natl Acad Sci USA* **114**, 438–447.
8 Hofmann S, Januliene D, Mehdipour AR, Thomas C, Stefan E, Bruchert S, Kuhn BT, Geertsma ER, Hummer G, Tampe R *et al.* (2019) Conformation space of a heterodimeric ABC exporter under turnover conditions. *Nature* **571**, 580–583.
9 Perez C, Gerber S, Boilevin J, Bucher M, Darbre T, Aebi M, Reymond JL and Locher KP (2015) Structure and mechanism of an active lipid-linked oligosaccharide flippase. *Nature* **524**, 433–438.
10 Perez C, Mehdipour AR, Hummer G and Locher KP (2019) Structure of outward-facing PglK and molecular dynamics of lipid-linked oligosaccharide recognition and translocation. *Structure* **27**, 669–678.e5.
11 Ward A, Reyes CL, Yu J, Roth CB and Chang G (2007) Flexibility in the ABC transporter MsbA:

alternating access with a twist. *Proc Natl Acad Sci USA* **104**, 19005–19010.
12 Mi W, Li YY, Yoon SH, Ernst RK, Walz T and Liao MF (2017) Structural basis of MsbA-mediated lipopolysaccharide transport. *Nature* **549**, 233–237.
13 Ho H, Miu A, Alexander MK, Garcia NK, Oh A, Zilberleyb I, Reichelt M, Austin CD, Tam C, Shriver S *et al*. (2018) Structural basis for dual-mode inhibition of the ABC transporter MsbA. *Nature* **557**, 196–201.
14 Johnson ZL and Chen J (2017) Structural basis of substrate recognition by the multidrug resistance protein MRP1. *Cell* **168**, 1075–1085.e9.
15 Johnson ZL and Chen J (2018) ATP binding enables substrate release from multidrug resistance protein 1. *Cell* **172**, 81–89.e10.
16 Lee JY, Yang JG, Zhitnitsky D, Lewinson O and Rees DC (2014) Structural basis for heavy metal detoxification by an Atm1-Type ABC exporter. *Science* **343**, 1133–1136.
17 Alam A, Kowal J, Broude E, Roninson I and Locher KP (2019) Structural insight into substrate and inhibitor discrimination by human P-glycoprotein. *Science* **363**, 753–756.
18 Lee JY, Kinch LN, Borek DM, Wang J, Wang J, Urbatsch IL, Xie XS, Grishin NV, Cohen JC, Otwinowski Z *et al*. (2016) Crystal structure of the human sterol transporter ABCG5/ABCG8. *Nature* **533**, 561–564.
19 Manolaridis I, Jackson SM, Taylor NMI, Kowal J, Stahlberg H and Locher KP (2018) Cryo-EM structures of a human ABCG2 mutant trapped in ATP-bound and substrate-bound states. *Nature* **563**, 426–430.
20 Bi Y, Mann E, Whitfield C and Zimmer J (2018) Architecture of a channel-forming O-antigen polysaccharide ABC transporter. *Nature* **553**, 361–365.
21 Gadsby DC, Vergani P and Csanady L (2006) The ABC protein turned chloride channel whose failure causes cystic fibrosis. *Nature* **440**, 477–483.
22 Aittoniemi J, Fotinou C, Craig TJ, de Wet H, Proks P and Ashcroft FM (2009) SUR1: a unique ATP-binding cassette protein that functions as an ion channel regulator. *Philos Trans Royal Soc B* **364**, 257–267.
23 Arnold FM, Weber MS, Gonda I, Gallenito MJ, Adenau S, Egloff P, Zimmermann I, Hutter CAJ, Hürlimann LM, Peters EE *et al*. (2020) The ABC exporter IrtAB imports and reduces mycobacterial siderophores. *Nature* **580**, 413–417.
24 Rempel S, Gati C, Nijland M, Thangaratnarajah C, Karyolaimos A, de Gier JW, Guskov A and Slotboom DJ (2020) A mycobacterial ABC transporter mediates the uptake of hydrophilic compounds. *Nature* **580**, 409–412.
25 Thomas C, Aller SG, Beis K, Carpenter EP, Chang G, Chen L, Dassa E, Dean M, Duong Van Hoa F, Ekiert D *et al*. (2020) Structural and functional diversity calls for a new classification of ABC transporters. *FEBS Lett* **594**, 3767–3775.
26 Bordignon E (2017) EPR spectroscopy of nitroxide spin probes. *eMagRes* **6**, 235–254.
27 Feintuch A, Otting G and Goldfarb D (2015) Gd(3+) spin labeling for measuring distances in biomacromolecules: why and how? *Methods Enzymol* **563**, 415–457.
28 Hubbell WL, McHaourab HS, Altenbach C and Lietzow MA (1996) Watching proteins move using site-directed spin labeling. *Structure* **4**, 779–783.
29 Bordignon E, Kucher S and Polyhach Y (2019) EPR techniques to probe insertion and conformation of spin-labeled proteins in lipid bilayers. *Methods Mol Biol* **2003**, 493–528.
30 Hubbell WL and Altenbach C (1994) Investigation of structure and dynamics in membrane proteins using site-directed spin labeling. *Curr Opin Strct Biol* **4**, 566–573.
31 Armstrong BD and Han S (2009) Overhauser dynamic nuclear polarization to study local water dynamics. *J Am Chem Soc* **131**, 4641–4647.
32 Jeschke G (2012) DEER distance measurements on proteins. *Annu Rev Phys Chem* **63**, 419–446.
33 Jeschke G (2018) The contribution of modern EPR to structural biology. *Emerg Top Life Sci* **2**, 9–18.
34 Ritsch I, Klose D, Hintz H, Godt A, Jeschke G and Yulikov M (2019) Pulsed EPR methods to study biomolecular interactions. *Chimia (Aarau)* **73**, 268–276.
35 Yulikov M (2015) Spectroscopically orthogonal spin labels and distance measurements in biomolecules. In Electron Paramagnetic Resonance (Chechik V, Murphy DM and Bruce G), Volume **24**, pp. 1–31. The Royal Society of Chemistry, London, UK.
36 Jeschke G (2018) MMM: a toolbox for integrative structure modeling. *Protein Sci* **27**, 76–85.
37 Yaginuma H, Kawai S, Tabata KV, Tomiyama K, Kakizuka A, Komatsuzaki T, Noji H and Imamura H (2014) Diversity in ATP concentrations in a single bacterial cell population revealed by quantitative single-cell imaging. *Sci Rep* **4**, 6522.
38 Timachi MH, Hutter CA, Hohl M, Assafa T, Böhm S, Mittal A, Seeger MA and Bordignon E (2017) Exploring conformational equilibria of a heterodimeric ABC transporter. *Elife* **6**, e20236.
39 Siarheyeva A, Liu R and Sharom FJ (2010) Characterization of an asymmetric occluded state of P-glycoprotein with two bound nucleotides: implications for catalysis. *J Biol Chem* **285**, 7575–7586.
40 Mittal A, Bohm S, Grutter MG, Bordignon E and Seeger MA (2012) Asymmetry in the homodimeric ABC transporter MsbA recognized by a DARPin. *J Biol Chem* **287**, 20395–20406.

41 Dong J, Yang G and McHaourab HS (2005) Structural basis of energy transduction in the transport cycle of MsbA. *Science* **308**, 1023–1028.
42 Barth K, Hank S, Spindler PE, Prisner TF, Tampe R and Joseph B (2018) Conformational coupling and trans-inhibition in the human antigen transporter ortholog TmrAB resolved with dipolar EPR spectroscopy. *J Am Chem Soc* **140**, 4527–4533.
43 Mishra S, Verhalen B, Stein RA, Wen PC, Tajkhorshid E and McHaourab HS (2014) Conformational dynamics of the nucleotide binding domains and the power stroke of a heterodimeric ABC transporter. *Elife* **3**, e02740.
44 Verhalen B, Dastvan R, Thangapandian S, Peskova Y, Koteiche HA, Nakamoto RK, Tajkhorshid E and McHaourab HS (2017) Energy transduction and alternating access of the mammalian ABC transporter P-glycoprotein. *Nature* **543**, 738–741.
45 Anderson MP, Rich DP, Gregory RJ, Smith AE and Welsh MJ (1991) Generation of cAMP-activated chloride currents by expression of CFTR. *Science* **251**, 679–682.
46 Chang G, Roth CB, Reyes CL, Pornillos O, Chen Y-J and Chen AP (2006) Retraction. *Science* **314**, 1875.
47 Borbat PP, Surendhran K, Bortolus M, Zou P, Freed JH and McHaourab HS (2007) Conformational motion of the ABC transporter MsbA induced by ATP hydrolysis. *PLoS Biol* **5**, e271.
48 Schultz KM, Merten JA and Klug CS (2011) Characterization of the E506Q and H537A dysfunctional mutants in the *E. coli* ABC transporter MsbA. *Biochemistry* **50**, 3599–3608.
49 Zou P, Bortolus M and McHaourab HS (2009) Conformational cycle of the ABC transporter MsbA in liposomes: detailed analysis using double electron-electron resonance spectroscopy. *J Mol Biol* **393**, 586–597.
50 Dawson RJ and Locher KP (2006) Structure of a bacterial multidrug ABC transporter. *Nature* **443**, 180–185.
51 Orelle C, Dalmas O, Gros P, Di Pietro A and Jault JM (2003) The conserved glutamate residue adjacent to the Walker-B motif is the catalytic base for ATP hydrolysis in the ATP-binding cassette transporter BmrA. *J Biol Chem* **278**, 47002–47008.
52 Liu Y, Liu Y, He L, Zhao Y and Zhang XC (2018) Single-molecule fluorescence studies on the conformational change of the ABC transporter MsbA. *Biophys Rep* **4**, 153–165.
53 Zou P and McHaourab HS (2010) Increased sensitivity and extended range of distance measurements in spin-labeled membrane proteins: Q-band double electron-electron resonance and nanoscale bilayers. *Biophys J* **98**, L18–L20.
54 Hellmich UA, Lyubenova S, Kaltenborn E, Doshi R, van Veen HW, Prisner TF and Glaubitz C (2012) Probing the ATP hydrolysis cycle of the ABC multidrug transporter LmrA by pulsed EPR spectroscopy. *J Am Chem Soc* **134**, 5857–5862.
55 Procko E, Ferrin-O'Connell I, Ng SL and Gaudet R (2006) Distinct structural and functional properties of the ATPase sites in an asymmetric ABC transporter. *Mol Cel* **24**, 51–62.
56 Collauto A, Mishra S, Litvinov A, McHaourab HS and Goldfarb D (2017) Direct spectroscopic detection of ATP turnover reveals mechanistic divergence of ABC exporters. *Structure* **25**, 1264–1274.e3.
57 Hrycyna CA, Ramachandra M, Ambudkar SV, Ko YH, Pedersen PL, Pastan I and Gottesman MM (1998) Mechanism of action of human P-glycoprotein ATPase activity. Photochemical cleavage during a catalytic transition state using orthovanadate reveals cross-talk between the two ATP sites. *J Biol Chem* **273**, 16631–16634.
58 Hohl M, Hurlimann LM, Bohm S, Schoppe J, Grutter MG, Bordignon E and Seeger MA (2014) Structural basis for allosteric cross-talk between the asymmetric nucleotide binding sites of a heterodimeric ABC exporter. *Proc Natl Acad Sci USA* **111**, 11025–11030.
59 Göddeke H, Timachi MH, Hutter CAJ, Galazzo L, Seeger MA, Karttunen M, Bordignon E and Schäfer LV (2018) Atomistic Mechanism of large-scale conformational transition in a heterodimeric ABC exporter. *J Am Chem Soc* **140**, 4543–4551.
60 Barth K, Rudolph M, Diederichs T, Prisner TF, Tampé R and Joseph B (2020) Thermodynamic basis for conformational coupling in an ATP-binding cassette exporter. *J Phys Chem Lett* **11**, 7946–7953.
61 Dastvan R, Mishra S, Peskova YB, Nakamoto RK and McHaourab HS (2019) Mechanism of allosteric modulation of P-glycoprotein by transport substrates and inhibitors. *Science* **364**, 689–692.
62 Aller SG, Yu J, Ward A, Weng Y, Chittaboina S, Zhuo R, Harrell PM, Trinh YT, Zhang Q, Urbatsch IL *et al.* (2009) Structure of P-glycoprotein reveals a molecular basis for poly-specific drug binding. *Science* **323**, 1718–1722.
63 Jin MS, Oldham ML, Zhang Q and Chen J (2012) Crystal structure of the multidrug transporter P-glycoprotein from *Caenorhabditis elegans*. *Nature* **490**, 566–569.
64 Mechetner EB and Roninson IB (1992) Efficient inhibition of P-glycoprotein-mediated multidrug resistance with a monoclonal antibody. *Proc Natl Acad Sci USA* **89**, 5824–5828.
65 Hamada H and Tsuruo T (1986) Functional role for the 170- to 180-kDa glycoprotein specific to drug-resistant tumor cells as revealed by monoclonal antibodies. *Proc Natl Acad Sci USA* **83**, 7785–7789.

66 Alam A, Kung R, Kowal J, McLeod RA, Tremp N, Broude EV, Roninson IB, Stahlberg H and Locher KP (2018) Structure of a zosuquidar and UIC2-bound human-mouse chimeric ABCB1. *Proc Natl Acad Sci USA* **115**, 1973–1982.
67 Ritchie TK, Kwon H and Atkins WM (2011) Conformational analysis of human ATP-binding cassette transporter ABCB1 in lipid nanodiscs and inhibition by the antibodies MRK16 and UIC2. *J Biol Chem* **286**, 39489–39496.
68 Hipolito CJ and Suga H (2012) Ribosomal production and *in vitro* selection of natural product-like peptidomimetics: the FIT and RaPID systems. *Curr Opin Struct Biol* **16**, 196–203.
69 Kodan A, Yamaguchi T, Nakatsu T, Sakiyama K, Hipolito CJ, Fujioka A, Hirokane R, Ikeguchi K, Watanabe B, Hiratake J *et al.* (2014) Structural basis for gating mechanisms of a eukaryotic P-glycoprotein homolog. *Proc Natl Acad Sci USA* **111**, 4049–4054.
70 Ward AB, Szewczyk P, Grimard V, Lee CW, Martinez L, Doshi R, Caya A, Villaluz M, Pardon E, Cregger C *et al.* (2013) Structures of P-glycoprotein reveal its conformational flexibility and an epitope on the nucleotide-binding domain. *Proc Natl Acad Sci USA* **110**, 13386–13391.
71 Seeger MA, Mittal A, Velamakanni S, Hohl M, Schauer S, Salaa I, Grütter MG and van Veen HW (2012) Tuning the drug efflux activity of an ABC transporter *in vivo* by *in vitro* selected DARPin binders. *PLoS One* **7**, e37845.
72 Perez C, Kohler M, Janser D, Pardon E, Steyaert J, Zenobi R and Locher KP (2017) Structural basis of inhibition of lipid-linked oligosaccharide flippase PglK by a conformational nanobody. *Sci Rep* **7**, 46641.
73 Zimmermann I, Egloff P, Hutter CA, Arnold FM, Stohler P, Bocquet N, Hug MN, Huber S, Siegrist M, Hetemann L *et al.* (2018) Synthetic single domain antibodies for the conformational trapping of membrane proteins. *eLife* **7**, e34317.
74 Zimmermann I, Egloff P, Hutter CAJ, Kuhn BT, Bräuer P, Newstead S, Dawson RJP, Geertsma ER and Seeger MA (2020) Generation of synthetic nanobodies against delicate proteins. *Nat Protoc* **15**, 1707–1741.
75 Galazzo L, Meier G, Timachi MH, Hutter CAJ, Seeger MA and Bordignon E (2020) Spin-labeled nanobodies as protein conformational reporters for electron paramagnetic resonance in cellular membranes. *Proc Natl Acad Sci USA* **117**, 2441–2448.
76 Geertsma ER, Nik Mahmood NAB, Schuurman-Wolters GK and Poolman B (2008) Membrane reconstitution of ABC transporters and assays of translocator function. *Nat Protoc* **3**, 256–266.
77 Ritchie TK, Grinkova YV, Bayburt TH, Denisov IG, Zolnerciks JK, Atkins WM and Sligar SG (2009) Reconstitution of membrane proteins in phospholipid bilayer nanodiscs. *Methods Enzymol* **464**, 211–231.
78 Arana MR, Fiori MC and Altenberg GA (2019) Functional and structural comparison of the ABC exporter MsbA studied in detergent and reconstituted in nanodiscs. *Biochem Biophys Res Commun* **512**, 448–452.
79 Efremov RG, Gatsogiannis C and Raunser S (2017) Lipid Nanodiscs as a tool for high-resolution structure determination of membrane proteins by single-particle Cryo-EM. *Methods Enzymol* **594**, 1–30.
80 Lacabanne D, Orelle C, Lecoq L, Kunert B, Chuilon C, Wiegand T, Ravaud S, Jault J-M, Meier BH and Böckmann A (2019) Flexible-to-rigid transition is central for substrate transport in the ABC transporter BmrA from *Bacillus subtilis*. *Commun Biol* **2**, 149.
81 Kaur H, Lakatos A, Spadaccini R, Vogel R, Hoffmann C, Becker-Baldus J, Ouari O, Tordo P, McHaourab H and Glaubitz C (2015) The ABC exporter MsbA probed by solid state NMR - challenges and opportunities. *Biol Chem* **396**, 1135–1149.
82 Hellmich UA, Haase W, Velamakanni S, van Veen HW and Glaubitz C (2008) Caught in the act: ATP hydrolysis of an ABC-multidrug transporter followed by real-time magic angle spinning NMR. *FEBS Lett* **582**, 3557–3562.
83 Kaur H, Lakatos-Karoly A, Vogel R, Nöll A, Tampé R and Glaubitz C (2016) Coupled ATPase-adenylate kinase activity in ABC transporters. *Nat Commun* **7**, 13864.
84 Wang L, Johnson ZL, Wasserman MR, Levring J, Chen J and Liu S. (2020) Characterization of the kinetic cycle of an ABC transporter by single-molecule and cryo-EM analyses. *eLife* **9**, e56451.
85 Husada F, Bountra K, Tassis K, de Boer M, Romano M, Rebuffat S, Beis K and Cordes T (2018) Conformational dynamics of the ABC transporter McjD seen by single-molecule FRET. *EMBO J* **37**, e100056.
86 Doshi R and van Veen HW (2013) Substrate binding stabilizes a pre-translocation intermediate in the ATP-binding cassette transport protein MsbA. *J Biol Chem* **288**, 21638–21647.
87 Qi M, Gross A, Jeschke G, Godt A and Drescher M (2014) Gd(III)-PyMTA label is suitable for in-cell EPR. *J Am Chem Soc* **136**, 15366–15378.
88 Azarkh M, Bieber A, Qi M, Fischer JWA, Yulikov M, Godt A and Drescher M (2019) Gd(III)-Gd(III) relaxation-induced dipolar modulation enhancement for in-cell electron paramagnetic resonance distance determination. *J Phys Chem Lett* **10**, 1477–1481.
89 Yulikov M, Lueders P, Warsi MF, Chechik V and Jeschke G (2012) Distance measurements in Au nanoparticles functionalized with nitroxide radicals

and Gd(3+)-DTPA chelate complexes. *Phys Chem Chem Phys* **14**, 10732–10746.
90 Lueders P, Jager H, Hemminga MA, Jeschke G and Yulikov M (2013) Distance measurements on orthogonally spin-labeled membrane spanning WALP23 polypeptides. *J Phys Chem B* **117**, 2061–2068.
91 Garbuio L, Bordignon E, Brooks EK, Hubbell WL, Jeschke G and Yulikov M (2013) Orthogonal spin labeling and Gd(III)-nitroxide distance measurements on bacteriophage T4-lysozyme. *J Phys Chem B* **117**, 3145–3153.
92 Garbuio L, Zimmermann K, Haussinger D and Yulikov M (2015) Gd(III) complexes for electron-electron dipolar spectroscopy: Effects of deuteration, pH and zero field splitting. *J Magn Reson* **259**, 163–173.
93 Yang Y, Yang F, Gong YJ, Chen JL, Goldfarb D and Su XC (2017) A reactive, rigid Gd(III) labeling tag for in-cell EPR Distance measurements in proteins. *Angew Chem Int Ed Eng* **56**, 2914–2918.
94 Theillet FX, Binolfi A, Bekei B, Martorana A, Rose HM, Stuiver M, Verzini S, Lorenz D, van Rossum M, Goldfarb D *et al.* (2016) Structural disorder of monomeric alpha-synuclein persists in mammalian cells. *Nature* **530**, 45–50.
95 Martorana A, Bellapadrona G, Feintuch A, Di Gregorio E, Aime S and Goldfarb D (2014) Probing protein conformation in cells by EPR distance measurements using Gd3+ spin labeling. *J Am Chem Soc* **136**, 13458–13465.
96 Yang Y, Chen S-N, Yang F, Li X-Y, Feintuch A, Su X-C and Goldfarb D (2020) In-cell destabilization of a homodimeric protein complex detected by DEER spectroscopy. *Proc Natl Acad Sci USA* **117**, 20566–20575.
97 Huang S, Paletta JT, Elajaili H, Huber K, Pink M, Rajca S, Eaton GR, Eaton SS and Rajca A (2017) Synthesis and xides. *J Org Chem* **82**, 1538–1544.
98 Paletta JT, Pink M, Foley B, Rajca S and Rajca A (2012) Synthesis and reduction kinetics of sterically shielded pyrrolidine nitroxides. *Org Lett* **14**, 5322–5325.
99 Wang Y, Paletta JT, Berg K, Reinhart E, Rajca S and Rajca A (2014) Synthesis of unnatural amino acids functionalized with sterically shielded pyrroline nitroxides. *Org Lett*. **16**, 5298–5300.
100 Huang S, Zhang H, Paletta JT, Rajca S and Rajca A (2018) Reduction kinetics and electrochemistry of tetracarboxylate nitroxides. *Free Radic Res* **52**, 327–334.
101 Bleicken S, Assafa TE, Zhang H, Elsner C, Ritsch I, Pink M, Rajca S, Jeschke G, Rajca A and Bordignon E (2019) gem-diethyl pyrroline nitroxide spin labels: synthesis, EPR characterization, rotamer libraries and biocompatibility. *ChemistryOpen* **8**, 1057–1065.
102 Jagtap AP, Krstic I, Kunjir NC, Hansel R, Prisner TF and Sigurdsson ST (2015) Sterically shielded spin labels for in-cell EPR spectroscopy: analysis of stability in reducing environment. *Free Radic Res* **49**, 78–85.
103 Weinrich T, Jaumann EA, Scheffer U, Prisner TF and Gobel MW (2018) A cytidine phosphoramidite with protected nitroxide spin label: synthesis of a full-length TAR RNA and investigation by in-line probing and EPR spectroscopy. *Chemistry* **24**, 6202–6207.
104 Weinrich T, Jaumann EA, Scheffer UM, Prisner TF and Gobel MW (2018) Phosphoramidite building blocks with protected nitroxides for the synthesis of spin-labeled DNA and RNA. *Beilstein J Org Chem* **14**, 1563–1569.
105 Karthikeyan G, Bonucci A, Casano G, Gerbaud G, Abel S, Thome V, Kodjabachian L, Magalon A, Guigliarelli B, Belle V *et al.* (2018) A bioresistant nitroxide spin label for in-cell EPR spectroscopy. *In vitro* and in oocytes protein structural dynamics studies. *Angew Chem Int Ed Engl* **57**, 1366–1370.
106 Schmidt MJ, Borbas J, Drescher M and Summerer D (2014) A genetically encoded spin label for electron paramagnetic resonance distance measurements. *J Am Chem Soc* **136**, 1238–1241.
107 Schmidt MJ, Fedoseev A, Bucker D, Borbas J, Peter C, Drescher M and Summerer D (2015) EPR distance measurements in native proteins with genetically encoded spin labels. *ACS Chem Biol* **10**, 2764–2771.
108 Schmidt MJ, Fedoseev A, Summerer D and Drescher M (2015) Genetically encoded spin labels for *in vitro* and in-cell EPR studies of native proteins. *Methods Enzymol* **563**, 483–502.
109 Kucher S, Korneev S, Tyagi S, Apfelbaum R, Grohmann D, Lemke EA, Klare JP, Steinhoff HJ and Klose D (2017) Orthogonal spin labeling using click chemistry for *in vitro* and *in vivo* applications. *J Magn Reson* **275**, 38–45.
110 Kucher S, Korneev S, Klare JP, Klose D and Steinhoff HJ (2020) In cell Gd(3+)-based site-directed spin labeling and EPR spectroscopy of eGFP. *Phys Chem Chem Phys* **22**, 13358–13362.
111 Widder P, Schuck J, Summerer D and Drescher M (2020) Combining site-directed spin labeling *in vivo* and in-cell EPR distance determination. *Phys Chem Chem Phys* **22**, 4875–4879.
112 Joseph B, Sikora A, Bordignon E, Jeschke G, Cafiso DS and Prisner TF (2015) Distance measurement on an endogenous membrane transporter in *E. coli* cells and native membranes using EPR spectroscopy. *Angew Chem Int Ed Engl* **54**, 6196–6199.
113 Joseph B, Tormyshev VM, Rogozhnikova OY, Akhmetzyanov D, Bagryanskaya EG and Prisner TF (2016) Selective high-resolution detection of membrane protein-ligand interaction in native membranes using

trityl-nitroxide PELDOR. *Angew Chem Int Ed Engl* **55**, 11538–11542.

114 Joseph B, Jaumann EA, Sikora A, Barth K, Prisner TF and Cafiso DS (2019) *In situ* observation of conformational dynamics and protein ligand-substrate interactions in outer-membrane proteins with DEER/PELDOR spectroscopy. *Nat Protocol* **14**, 2344–2369.

115 Nyenhuis DA, Nilaweera TD, Niblo JK, Nguyen NQ, DuBay KH and Cafiso DS (2020) Evidence for the supramolecular organization of a bacterial outer-membrane protein from *in vivo* pulse electron paramagnetic resonance spectroscopy. *J Am Chem Soc* **142**, 10715–10722.